American Journal of Pathology, Vol. 150, No. 2, February 1997

Role of Nitric Oxide in Tumor Microcirculation

Blood Flow, Vascular Permeability, and Leukocyte-Endothelial Interactions

Dai Fukumura, Fan Yuan, Mitsuhiro Endo, and Rakesh K. Jain

From the Edwin L. Steele Laboratory, Department of Radiation Oncology, Massachusetts General Hospital and Harvard Medical School, Boston, Massachusetts

The present study was designed to define the role of nitric oxide (NO) in tumor microcirculation, through the direct intravital microcirculatory observations after administration of NO synthase (NOS) inhibitor and NO donor both regionally and systemically. More specifically, we tested the following hypotheses: 1) endogenous NO derived from tumor vascular endothelium and/or tumor cells increases and/or maintains tumor blood flow, decreases leukocyte-endothelial interactions, and increases vascular permeability, 2) exogenous NO can increase tumor blood flow via vessel dilatation and decrease leukocyte-endothelial interactions, and 3) NO production and tissue responses to NO are tumor dependent. To this end, a murine mammary adenocarcinoma (MCaIV) and a human colon adenocarcinoma (LS174T) were implanted in the dorsal skinfold chamber in C3H and severe combined immunodeficient mice, respectively, and observed by means of intravital fluorescence microscopy. Both regional and systemic inhibition of endogenous NO by Nω-nitro-L-arginine methyl ester (L-NAME; 100 μmol/L superfusion or 10 mg/kg intravenously) significantly decreased vessel diameter and local blood flow rate. The diameter change was dominant on the arteriolar side. Superfusion of NO donor (spermine NO, 100 μmol/L) increased tumor vessel diameter and flow rate, whereas systemic injection of spermine NO (2.62 mg/kg) had no significant effect on these parameters. Rolling and stable adhesion of leukocytes were significantly increased by intravenous injection of L-NAME. In untreated animals, both MCaIV and LS174T tumor vessels were leaky to albumin. Systemic NO inhibition significantly attenuated tumor vascular permeability of MCaIV but not of LS174T tumor. Immunohistochemical studies, using polyclonal antibodies to endothelial NOS and inducible NOS, revealed a diffuse pattern of positive labeling in both MCaIV and LS174T tumors. Nitrite and nitrate levels in tumor interstitial fluid of MCaIV but not of LS174T were significantly higher than that in normal subcutaneous interstitial fluid. These results support our hypotheses regarding the microcirculatory response to NO in tumors. Modulation of NO level in tumors is a potential strategy for altering tumor hemodynamics and thus improving oxygen, drug, gene vector, and effector cell delivery to solid tumors. (Am J Pathol 1997, 150:713–725)

Nitric oxide (NO) is a molecule with extremely high reactivity and a variety of physiological activities.[1] There are three isoforms of NO synthase (NOS): endothelial (eNOS), neuronal (nNOS), and inducible (iNOS). NO released from endothelial cells is considered to act cytoprotectively because of its ability to improve blood flow through relaxation of vascular smooth muscle cells,[2,3] inhibition of platelet aggregation,[4] elimination of free radicals,[5] inhibition of leukocyte adhesion to the vascular endothelium,[3] and leukocyte migration

Supported by an Outstanding Investigator Grant from the National Cancer Institute (R35-CA56591) to R. K. Jain. D. Fukumura is a Whitaker fellow.

Accepted for publication October 10, 1996.

Address reprint requests to Dr. Rakesh K. Jain, Department of Radiation Oncology, Massachusetts General Hospital, Boston, MA 02114.

Table 1. *Role of NO in Tumor Microcirculation*

Tumor	Methods	Treatment	Results	Reference
Hemodynamics				
Colon 26 B16 melanoma	Xe injection	L-NAME (3–30 μg i.t.) L-NMMA	TBF ↓	9
KHT sarcoma RIF-1 sarcoma SCCVII/Ha carcinoma	MRS	L-NNA (0.01–20 mg/kg i.v.)	pO_2 ↓	10
P22 carcinosarcoma	[^{125}I]IAP injection, *ex vivo* perfusion	L-NNA (10 mg/kg i.v.) L-NNA (1–100 μmol/L) Sodium nitroprusside (0.5–100 μmol/L)	TBF ↓ by L-NNA Resistance ↓ by NO	11
R3230Ac Mammary adenocarcinoma	Intravital microscope	L-NMMA (50 μmol/L)	VRBC/diameter ↓	12
MCaIV Mammary adenocarcinoma LS174T Human colon adenocarcinoma	Intravital microscope	L-NAME (100 μmol/L) (10 mg/kg i.v.) SNO (100 μmol/L) (10 μmol/kg i.v.)	Reg: diameter/flow ↓ by L-NAME diameter ↑ by NO Syst: diameter/flow ↓ by L-NAME NO donor, no effect	This work
Leukocyte-endothelial interaction				
MCaIV	Intravital microscope	L-NAME (10 mg/kg i.v.)	Flux: no change Rolling ↑ Adhesion ↑	This work
Vascular permeability				
Sarcoma-180	Evans blue exclusion	L-NAME (4.2 mg/kg i.p.) PTIO (21.5 μmol)	Permeability ↓	13
RG2 glioma	Autoradiography	BK + L-NAME (6 mg/kg i.v.)	BK-induced permeability change ↓	28
MCaIV LS174T	Intravital microscope	L-NAME (10 mg/kg i.v.)	MCaIV ↓ LS174T: no change	This work

TBF, tumor blood flow; L-NMMA, N^G-monomethyl-L-arginine; i.t., intra tumor injection; i.v., intravenous injection; MRS, ^{31}P magnetic resonance spectroscopy; L-NNA, $N\omega$-nitro-L-arginine; SNO, spermine NO; Reg, regional treatment; Syst, systemic treatment; PTIO, 2-phenyl-4,4,5,5-tetramethylimidazoline-1-oxyl-3-oxide; BK, bradykinin.

through blood vessel wall.[6] On the other hand, NO and its metabolites released by activated macrophages[7] or Kupffer cells[8] are cytotoxic and cause dysfunction of mitochondria in tumor cells.

Knowledge about NO in tumor microcirculation is limited compared with that in normal tissues (Table 1). Andrade et al[9] reported that inhibition of endogenous NOS reduced tumor blood flow. Wood et al[10] showed that inhibition of NOS induced hypoxia in murine tumors. Tozer et al[11] reported that NOS inhibitor increased the vascular resistance of perfused tumors. Recently, Meyer et al[12] found that NOS inhibition irreversibly decreased tumor perfusion. Thus, NO may play a role in maintaining tumor blood flow and nutrient supply. Maeda et al[13] showed that NO inhibition reduced extravasation of Evans blue dye in tumor tissue. Based on these published data in normal and tumor tissues, we hypothesize that 1) endogenous NO derived from tumor vascular endothelium and/or tumor cells increases and/or maintains tumor blood flow, decreases leukocyte-endothelial interactions, and increases vascular permeability, 2) exogenous NO can increase tumor blood flow *via* vessel dilatation and decrease leukocyte-endothelial interactions, and 3) NO production and tissue responses to NO are tumor dependent.

The present study was designed to test the above hypotheses and to define the role of NO in tumor microcirculation. Through the use of NOS inhibitor and NO donor, both regionally and systemically, we determined 1) the effect of inhibition of endogenous NO on tumor blood flow, vascular diameter, leukocyte-endothelial interactions, and vascular permeability, and 2) the effect of exogenous NO on microcirculatory hemodynamics and leukocyte-endothelial interactions in a murine tumor (MCaIV) and a human tumor xenograft (LS174T). We also determined the production of NO in tumor tissue by measuring nitrite and nitrate levels in tumor interstitial fluid (TIF) and the local-

ization of endothelial and inducible types of NOS using anti-NOS antibodies.

Materials and Methods

Animals, Surgery, and Tumor Implantation

Dorsal skin chambers were implanted in mice using the procedure described previously.[14,15] Two-month-old C3H and severe combined immunodeficient (SCID) mice (25 to 30 g) were used. A chunk (1 mm in diameter) of MCaIV (a murine mammary adenocarcinoma) or 2 μl of dense LS174T (a human colon adenocarcinoma) cell suspension ($\sim 2 \times 10^5$ cells) was implanted at the center of the dorsal chamber. MCaIV was implanted in C3H mice. LS174T was implanted in SCID mice. The measurements were made between 8 and 12 days for MCaIV and 21 and 28 days for LS174T when tumors were approximately 3×3 mm^2 in surface area.

Tracers

Tetramethylrhodamine-labeled bovine serum albumin (Rho-BSA; Molecular Probes, Eugene, OR) and cyanine-5-labeled BSA (Cy5-BSA) were used as tracers for permeability studies. Cy5-succinimidyl esters (Amersham, Arlington Heights, IL) was conjugated to BSA (Sigma Chemical Co., St. Louis, MO) with the modified method of Southwick et al.[16] Rho-BSA and Cy5-BSA were dissolved in phosphate-buffered saline (PBS) at a concentration of 10 mg/ml. The free fluorescent dye in the solution was removed by passing through a size exclusion column. Rhodamine 6G (Rho-6G; Molecular Probes) was used for *in situ* labeling of leukocytes.[17] Rho-6G was dissolved in PBS at a concentration of 1 mg/ml. Solutions of these fluorescent dye were passed through a 0.2-μm filter before injection.

Agents Studied

To inhibit the production of endogenous NO in tumor, *N*ω-nitro-L-arginine-methyl ester (L-NAME; Sigma), an inhibitor of NOS, was added to the superfusate at a concentration of 100 μmol/L or injected systemically (10 mg/kg) *via* tail vein. Sixty minutes after the superfusion of L-NAME, the superfusate was changed to L-arginine (200 μmol/L) in Hank's balanced salt solution (HBSS; Sigma). In other series of experiments, spermine NO (RBI, Natick, MA) was used as exogenous NO to tumors. Spermine NO was added to superfusate at a concentration of 100 μmol/L or injected systemically (2.62 mg/kg) *via* tail vein.

Experimental Procedure

The animals were anesthetized with a subcutaneous injection of a cocktail of 90 mg of Ketamine (Parke-Davis, Morris Plains, NJ) and 9 mg of Xylazine (Fermenta, Kansas City, MO) per kilogram of body weight. The mice were positioned in a polycarbonate tube and the chamber was fixed on the microscope stage. For regional treatment, the coverslip was removed and the surface of the tumor was continuously superfused with HBSS at 1 ml/minute bubbled with 95% N_2 and 5% CO_2 and prewarmed in water-bath at 37°C. To obtain microcirculatory parameters, randomly selected areas (three to six locations per animal) of the tumor were investigated using a 20× water immersion objective (for regional treatment) or a 20× long-working-distance objective (for systemic treatment) and an intravital fluorescence microscope (Axioplan, Zeiss, Oberkochen, Germany) equipped with the fluorescence filter sets for Rho and Cy5 (Omega Optical, Brattleboro, VT), an intensified charge-coupled device (CCD) video camera (C2400-88, Hamamatsu Photonics K.K., Hamamatsu, Japan), a regular CCD video camera (AVC-D7, Sony, Tokyo, Japan), a photomultiplier (9203B, EMI, Rockaway, NJ), and a S-VHS videocassette recorder (SVO-9500MD, Sony). To minimize the variation in microvascular parameters of tumor vessels as described previously,[14] the same preselected vessels were observed for each experiment and the relative changes from their baseline values were reported. To facilitate the localization of preselected vessels, tumor images were recorded at a lower magnification using a thermal video printer (P67U, Mitsubishi, Somerset, NJ).

In each observation, transilluminated tissue images were recorded for 60 seconds and the video tapes were analyzed off-line as follows. The vessel diameter in microns (D) was measured using an image-shearing device (digital video image shearing monitor, model 908, IPM, San Diego, CA). The red blood cell velocity (V_{RBC}) was measured using the four-slit apparatus (Microflow System, model 208C, video photometer version, IPM) equipped with a personal computer (IBM PS/2, 40SX, Computerland, Boston, MA). The mean blood flow rates of individual vessels (Q) were calculated using D and the mean V_{RBC} (V_{mean}) as follows: $Q = \pi/4 \times V_{mean} \times D^2$; $V_{mean} = V_{RBC}/\alpha$ ($\alpha = 1.3$, for blood vessels <10 μm; by linear extrapolation, $1.3 < \alpha < 1.6$ for blood

vessels between 10 and 15 μm; and α = 1.6 for blood vessels >15 μm).[18]

In case of systemic application of agents, systemic arterial blood pressure was monitored. The neck of the animal was shaved, and an incision was made above the right carotid artery. The catheter (PE10, Becton Dickinson, Sparks, MD) filled with physiological saline and heparin was inserted into the carotid artery. The distal end of the catheter was connected to a pressure transducer (P23XL, Spectramed, Oxnard, CA). The pressure transducer was linked to a preamplifier (Gould, Cleveland, OH) and the signal was sent to an analog-to-digital converter (MacLab 4, World Precision Instruments, Sarasota, FL) linked to a computer (Macintosh Classic II, Apple Computer, Cupertino, CA).

Leukocyte-endothelial interactions in tumor vessels were monitored as described previously.[15] Briefly, mice were injected with a bolus (20 μl) of 0.1% Rho-6G (excitation peak at 528 nm, emission peak at 550 nm) in 0.9% saline through the tail vein and leukocytes were visualized *via* an intensified CCD camera and recorded on a S-VHS tape. The numbers of rolling (N_r) and adhering (N_a) leukocytes were counted for 30 seconds along a 100-μm segment of a vessel. The total flux of cells for 30 seconds was also measured (N_t). The ratio of rolling cells to total flux (rolling count) was calculated as follows: rolling count (percent) = $100 \times N_r/N_t$. The density of adhering leukocytes was calculated as follows: density (cells/mm^2) = $10^6 \times N_a/(\pi \times D \times 100\ \mu m)$. Shear rate was calculated for each vessel as: shear rate = $8 \times V_{mean}/D$.

To determine the changes in vascular permeability, two different color fluorescent tracers were used at the same location. To minimize the light absorption by hemoglobin, long-wavelength tracers were used. Rho-BSA (excitation peak at 541 nm, emission peak at 572 nm) was used for baseline measurements and Cy5-BSA (excitation peak at 649 nm, emission peak at 670 nm) was used for post-treatment measurements. After the injection of tracer molecules (0.1 ml/25 g body weight), the fluorescence intensity of the tumor tissue was intermittently measured for 20 minutes. To minimize heterogeneity of vascular structure, we measured the effective vascular permeability (P) as described previously.[19,20] In brief, the equation to estimate P is: $P = (1 - Ht)\ V/S\ \{1/(I_0 - I_b) \times dI/dt + 1/K\}$ derived by Yuan et al,[20] where I is the average fluorescence intensity of the whole image, I_0 is the value of I immediately after the filling of all vessels by Rho-BSA or Cy5-BSA, and I_b is the background fluorescence intensity. The average hematocrit (Ht) of tumor vessels was assumed to be equal to 19%.[21] V and S are the total volume and surface area of vessels within the tissue volume covered by the surface image, respectively. The time constant of BSA plasma clearance (K) was 9.1×10^3 seconds.[19]

Immunohistochemistry

For immunohistochemical observations, additional tumors (six MCaIV and six LS174T) were transplanted in the dorsal skin chambers by the method described above. Tumor tissue blocks were fixed by 2% paraformaldehyde, 75 mmol/L lysine, and 10 mmol/L sodium periodate for 3 hours, infiltrated with 30% sucrose overnight, mounted in OCT medium (Miles, Elkhart, IN), frozen in liquid nitrogen, and sectioned serially at 5 μm thickness on a Reichert Frigocut cryostat. Sections were immunolabeled by an indirect fluorescence method.[22] To detect the localization of NOS, rabbit anti-eNOS and anti-iNOS polyclonal antibodies (Transduction Laboratories, Lexington, KY) were used as the primary antibodies and Cy3-conjugated donkey anti-rabbit IgG (Jackson ImmunoResearch Laboratories, West Grove, PA) was used as the secondary antibody. For endothelial cell and macrophage labeling, rat anti-murine CD31 monoclonal antibody MEC13.3 and rat anti-Mac 3 monoclonal antibody M3/84 (PharMingen, San Diego, CA) were used as the primary antibodies and Cy3-conjugated donkey anti-rat IgG (Jackson ImmunoResearch Laboratories) was used as the secondary antibody. Sections were examined with a light microscope (Microphot FXA, Nikon, Tokyo, Japan) equipped for epifluorescence and photographed using a Kodak TMAX 400 ASA film push-processed to 1600 ASA.

Nitrite and Nitrate Measurement

To determine the amount of NO production in solid tumors, nitrite and nitrate levels in interstitial fluid collected from Gullino's chamber,[23] implanted with MCaIV or LS174T tumors or without any tumor in mice, were measured. Plasma from these mice was also collected and analyzed for nitrite and nitrate levels. To remove proteins that might interfere with the measurement, samples were placed into a microfilter tube, with a molecular weight cut-off size of 10,000 (Microcon 10, Amicon, Beverly, MA) and centrifuged for 20 minutes (Centrifuge 5414, Eppendorf, Hamburg, Germany) before the measurement. Nitrite and nitrate levels were measured by photometric assay using Griess reagent after the conversion of

nitrate to nitrite utilizing nitrate reductase (nitrate/nitrite assay kit, Cayman Chemical, Ann Arbor, MI).

Statistical Methods

The data were analyzed using an analysis of variance and the Fisher's *post hoc* test. Values are expressed as mean ± SD unless specified. Statistical significance was set at $P < 0.05$.

Results

Hemodynamic Parameters: Regional Treatment

MCaIV Tumors

A 60-minute superfusion with HBSS did not cause any significant change in vessel diameter, V_{RBC} and calculated blood flow rate (Figure 1).

L-NAME (100 μmol/L superfusion), an inhibitor of NO synthesis, significantly decreased vessel diameter, V_{RBC}, and calculated blood flow rate in comparison with HBSS control (Figure 1). After 60 minutes of L-NAME superfusion, superfusate was changed to HBSS containing L-arginine (200 μmol/L). After an additional 60 minutes of L-arginine superfusion, vascular diameter, V_{RBC}, and flow recovered to 96.2 ± 12.0%, 85.7 ± 20.3%, and 86.5 ± 31.2% of the baselines, respectively. To understand the mechanisms behind the observation, these data were further divided into two groups: arteriolar side and venular side. Arteriolar vessels were defined as branching vessels entering the tumor surface from the periphery or underneath of the tumor. The remaining vessels, including capillary or venule-like vessels, were considered as venular ones. The changes in vessel diameter after L-NAME superfusion were more pronounced in arteriolar vessels, whereas the changes in V_{RBC} were more pronounced in venular vessels (Figure 1). The changes in calculated blood flow rate were comparable in both types of vessels.

Spermine NO (100 μmol/L superfusion), a donor of NO, significantly increased vessel diameter (113.6 ± 10.8% at 15 minutes and 106.8 ± 3.4% at 30 minutes) and local blood flow rate (133.6 ± 19.5% at 15 minutes and 118.6 ± 17.7% at 30 minutes) but not V_{RBC} when applied regionally (Figure 1).

LS174T Tumors

L-NAME (100 μmol/L) superfusion significantly decreased vessel diameter, V_{RBC}, and calculated flow rate (Figure 1). Similar to MCaIV tumors, the changes in vessel diameter were dominant in arteriolar vessels.

Hemodynamic Parameters: Systemic Treatment

MCaIV Tumors

Systemic injection of saline did not change significantly arterial blood pressure and hemodynamic parameters in tumor vessels. Intravenous injection of 10 mg/kg L-NAME caused a significant and sustained increase in arterial blood pressure (164.2% at 5 minutes and 159.8% at 60 minutes) and significant decrease in vessel diameter, V_{RBC}, and blood flow rate (Figure 2). Systemic injection of spermine NO (2.62 mg/kg) led to a rapid decrease in blood pressure (73.3% at 5 minutes) initially; then the pressure recovered to 83.9% at 60 minutes. Systemic injection of NO donor induced no significant change in hemodynamic parameters in tumor vessels.

LS174T Tumors

Systemic injection of L-NAME mainly reduced arteriolar vessels' diameter and V_{RBC} in venular vessels. Calculated blood flow rate also decreased, which was comparable in both types of vessels. The hemodynamic changes in MCaIV and LS174T tumors after L-NAME injection were consistent.

Leukocyte-Endothelial Interactions

In leukocyte-endothelial interaction studies, only venular vessels were examined. Leukocyte flux was heterogeneous among tumor vessels and did not show any significant response to any treatment. On the other hand, leukocyte rolling and adhesion in both MCaIV and LS174T tumor vessels were significantly increased in a time-dependent manner after the systemic injection of L-NAME (Figure 3). Leukocyte rolling tended to decrease after spermine NO injection but this change was not statistically significant.

Vascular Permeability

Similar to our previous observation,[19,20] both MCaIV and LS174T tumors were leaky to BSA. Baseline effective permeability was comparable between these two tumors. Inhibition of endogenous NO by systemic L-NAME injection significantly decreased vascular permeability of MCaIV tumors (Figure 4). Vessel permeability of LS174T tumors tended to de-

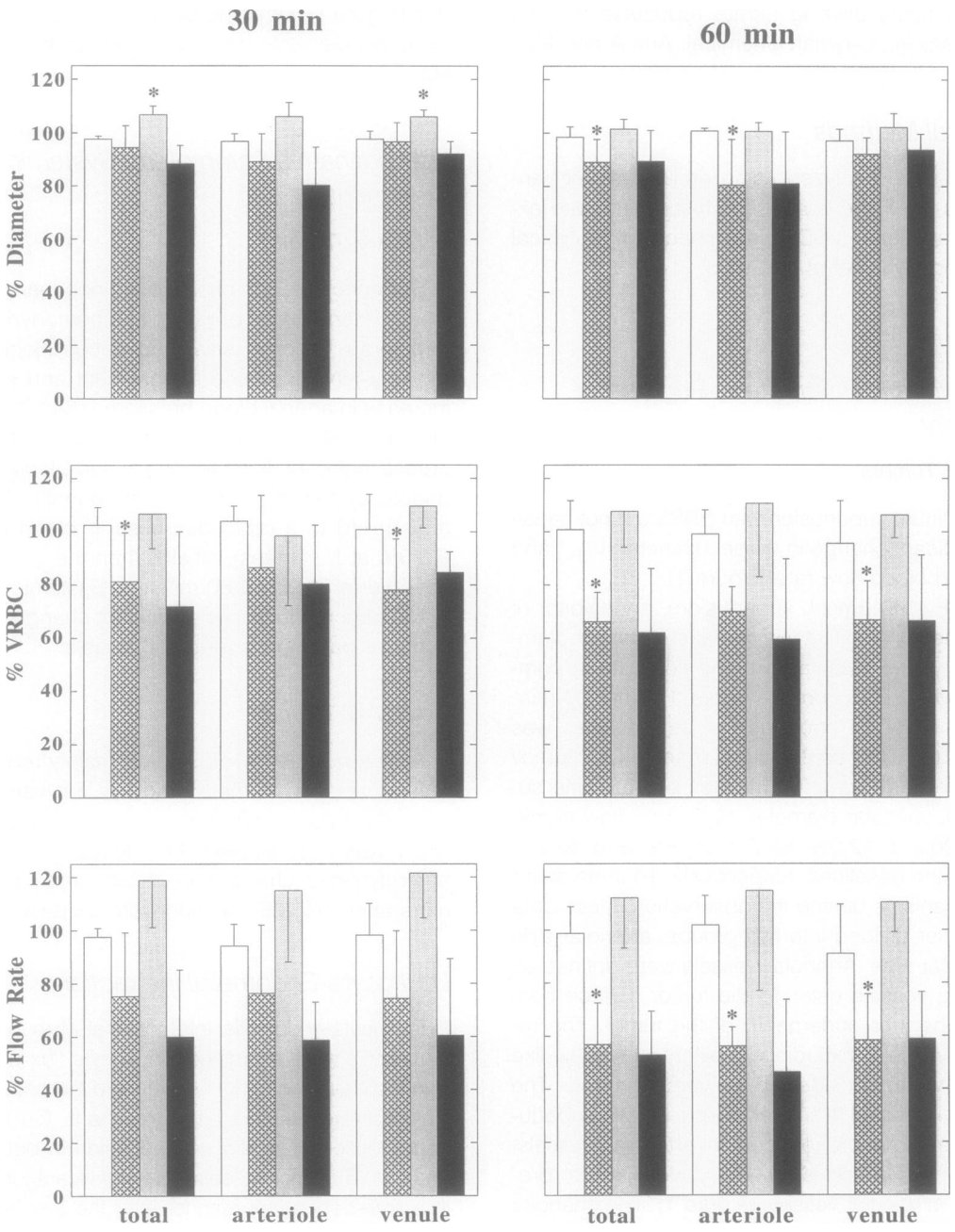

Figure 1. *Relative changes in hemodynamic parameters after regional treatment. MCaIV tumors were superfused with either HBSS only (□, n = 5), 100 μmol/L L-NAME in HBSS (▩, n = 5), or 100 μmol/L spermine NO in HBSS (▨, n = 5). LS174T tumors were superfused with 100 μmol/L L-NAME in HBSS (■, n = 5). Relative values (percent) with respect to corresponding baseline values at 30 minutes and 60 minutes after the start of superfusion were calculated. Data were first analyzed including all vessels observed (total) and then divided into two groups: arteriolar side (arteriole) and venular side (venule). L-NAME significantly decreased vessel diameter, V_{RBC}, and calculated blood flow rate. Data are presented as mean ± SD. *P < 0.05 (a significant difference) with respect to corresponding value of the control group.*

crease after L-NAME treatment, but this change was not statistically significant.

Immunohistochemistry

Immunolabeling with a polyclonal antibody to eNOS revealed a diffuse pattern of positive staining in both MCaIV and LS174T tumors (Figure 5, A and D). Immunolabeling with a polyclonal antibody to iNOS revealed a diffuse staining that was slightly stronger than eNOS in both tumors (Figure 5, B and E). CD31 staining for vascular endothelial cells was positive in both tumors (Figure 5, C and F). In MCaIV tumors, Mac-3 staining was nearly negative, although there

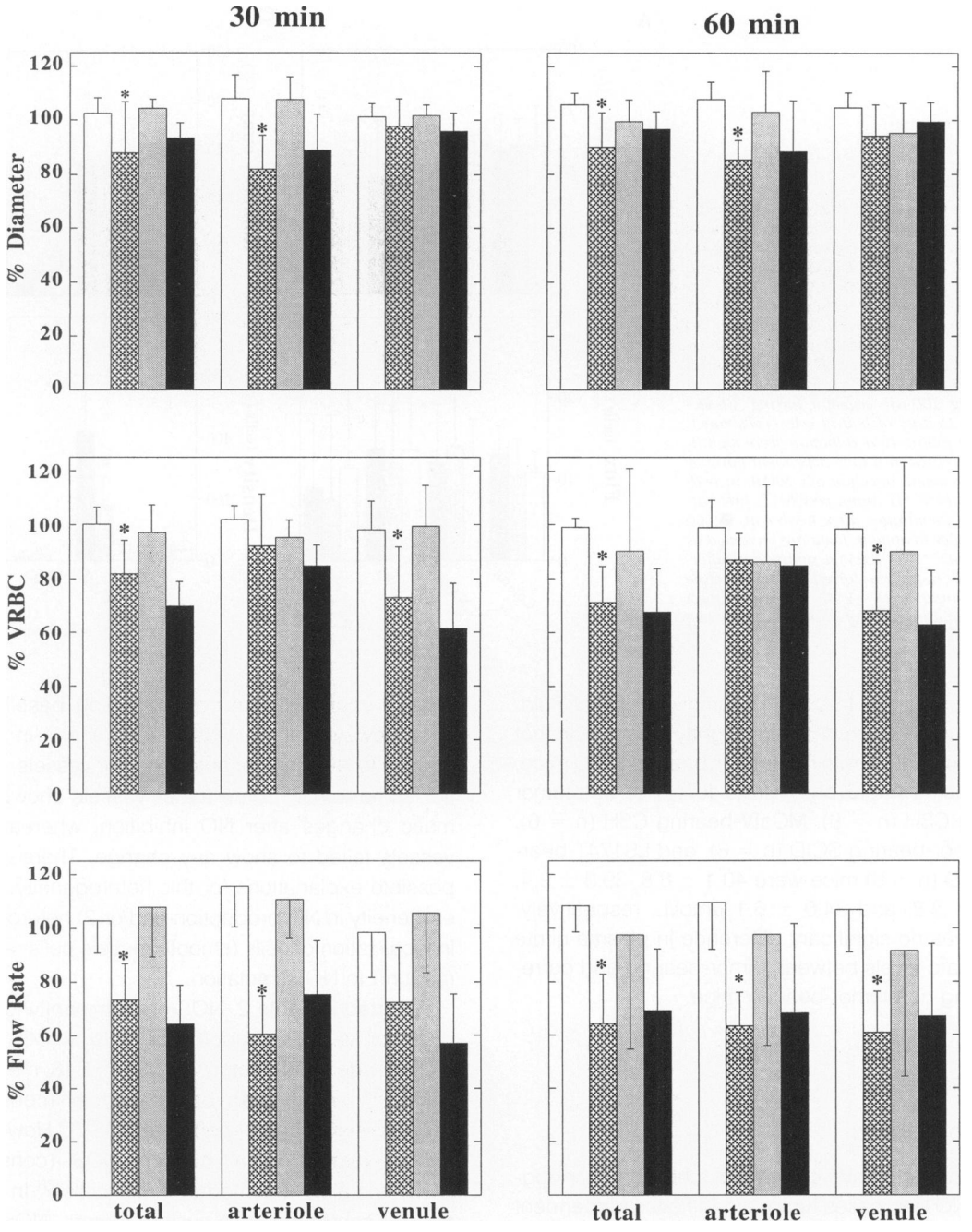

Figure 2. *Relative changes in hemodynamic parameters after systemic treatment. MCaIV tumor-bearing mice were injected with either physiological saline (□, n = 6), 10 mg/kg L-NAME (▩, n = 9), or 2.62 mg/kg spermine NO (▨, n = 7). LS174T tumor-bearing mice were injected with 10 mg/kg L-NAME (■, n = 5). Relative values (percent) with respect to corresponding baseline values at 30 minutes and 60 minutes after the injection were calculated. Data are presented identical to Figure 1.*

was a patchy positive staining in LS174T tumors (data not shown). The patterns of immunolabeling for both NOS types in tumors were completely different from that of CD31 or Mac-3, suggesting the expression of both NOSs by tumor cells.

Nitrite and Nitrate Levels

Nitrite and nitrate levels in MCaIV tumor interstitial fluid were significantly higher than that in subcutaneous interstitial fluid from non-tumor-bearing C3H

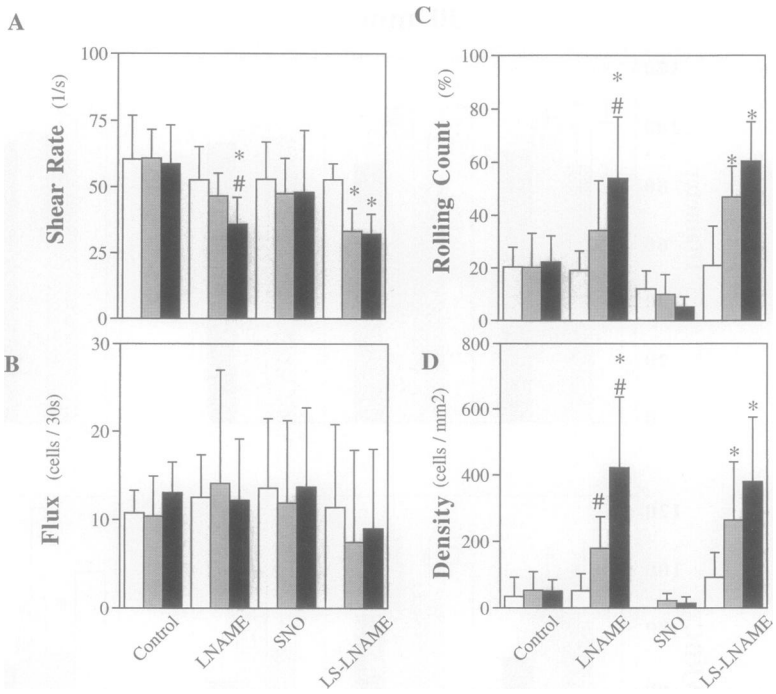

Figure 3. *Alteration in leukocyte-endothelial interactions in tumor vessels during NO modulation. MCaIV tumor-bearing mice were injected with either physiological saline (control, n = 6), 10 mg/kg L-NAME (LNAME, n = 6), or 2.62 mg/kg spermine NO (SNO, n = 5). LS174T tumor-bearing mice were injected with 10 mg/kg L-NAME (LS-LNAME, n = 5).* **A:** *Shear rate.* **B:** *Leukocyte flux.* **C:** *Rolling count (100 × number of rolling cells/total number of cells along 100-μm segment during 30 seconds).* **D:** *Density of bound cells (cells/mm²). Leukocyte rolling and adhesion were significantly increased in a time-dependent manner after the systemic injection of L-NAME in both MCaIV and LS174T tumor vessels. □, pretreatment; ▨, 30 minutes after treatment; ■, 60 minutes after treatment. Data are presented as mean ± SD. *P < 0.05 (a significant difference) with respect to corresponding baseline value (pretreatment). #P < 0.05 with respect to corresponding value of saline-injected group (control).*

mice (Figure 6). In LS174T tumor interstitial fluid, nitrite and nitrate levels were slightly higher than that in interstitial fluid from non-tumor-bearing SCID mice. The plasma nitrite and nitrate levels of non-tumor bearing C3H (n = 6), MCaIV-bearing C3H (n = 6), non-tumor-bearing SCID (n = 6), and LS174T-bearing SCID (n = 6) mice were 40.1 ± 8.8, 39.3 ± 9.4, 26. 9 ± 3.8, and 34.0 ± 6.1 μmol/L, respectively. There was no significant difference in plasma nitrite and nitrate levels between tumor-bearing and corresponding non-tumor-bearing mice.

Discussion

Hemodynamics

Studies to date have shown that inhibition of endogenous NO decreases tumor blood flow, independent of tumor type or method of measurement used (Table 1).[9–12] In this study, we demonstrated that tumor blood flow decreased after both regional and systemic treatments with NOS inhibitor. Both regional and systemic inhibition of endogenous NO significantly decreased vessel diameter mainly on the arteriolar side and V_{RBC} mainly on venular side in both murine MCaIV and human LS174T tumors. As a result, calculated blood flow rate was significantly decreased in both tumors. Statistical comparison of the hemodynamic response to NO inhibitor between these two tumors showed no difference in terms of relative changes from corresponding baseline values. However, there was heterogeneity in the response to NO inhibitor among tumor vessels, even in the same tumor. Some tumor vessels showed dramatic changes after NO inhibition, whereas other vessels failed to show any change. There are two possible explanations for this heterogeneity: 1) heterogeneity in NO production and/or 2) heterogeneity in localization of cells (smooth muscle cells, etc) that respond to NO stimulation.

As listed in Table 2, NOS predominantly localizes in tumor vascular endothelial cells in COLON 26 murine adenocarcinoma (iNOS),[24] B16 melanoma (iNOS),[24] and human breast cancer (constitutive NOS, ie, eNOS and/or neuronal NOS).[25] However, in human gynecological cancer, NOS (constitutive NOS) is mainly detected in tumor cells.[26] In human and rat central nervous system tumors, NOS is detected in both tumor cells (nNOS and eNOS) and endothelial cells (eNOS).[27,28] These findings suggest that localization of NOS is tumor dependent and that there is no correlation between the NOS type and cell types. As a result, the response to NO inhibitor is likely to be heterogeneous and tumor dependent. However, in this study, immunolabeling with anti-NOS antibodies revealed a diffuse staining for both eNOS and iNOS in both MCaIV and LS174T tumors, suggesting a uniform distribution of both NOSs in our tumor models.

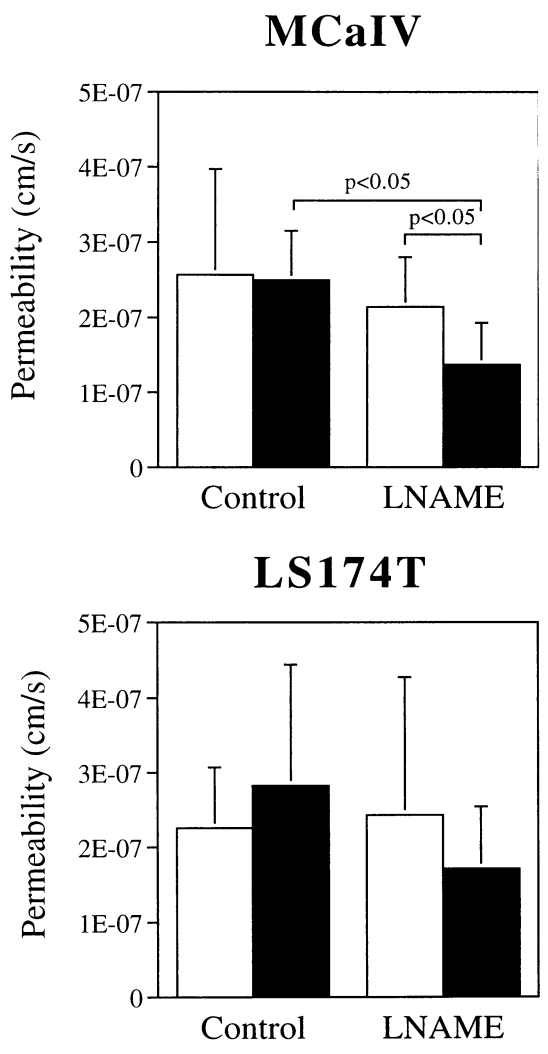

Figure 4. *Vascular permeability of MCaIV and LS174T tumors: effect of NO inhibition. Both MCaIV-bearing and LS174T-bearing mice were injected with saline (control) or 10 mg/kg L-NAME (LNAME). L-NAME injection significantly decreased vascular permeability of MCaIV but not LS174T tumors. □, pretreatment; ■, 60 minutes after treatment. Data are presented as mean ± SD. (MCaIV control, n = 8; MCaIV L-NAME, n = 10; LS174T control, n = 7; LS174T L-NAME, n = 7).*

Lack of functional smooth muscle cells in tumors has been reported in the literature.[29,30] Tanda et al reported that there were a few smooth muscle α-actin-positive cells in the peripheral region of tissue-isolated tumors and almost no smooth muscle α-actin-positive cells inside tumors.[31] The lack of smooth muscle cells or other contractile cells along tumor vessels could be a possible reason for the heterogeneous response to NO treatment. In this study, arteriolar vessels, which are mainly located in the periphery of tumors, showed significant changes in vessel diameter after NO inhibition, indicating that arteriolar vessels in tumors are likely to have more contractile cells than venular vessels and thus may play an important role in control of tumor blood flow.

Although superfusion of NO donor increased tumor vessel diameter and blood flow rate to some extent, these changes were not statistically significant. Furthermore, systemic treatment of NO donor failed to increase tumor blood flow. The decrease in systemic blood pressure might explain this difference. The hemodynamic response to additional exogenous NO seemed to be limited, presumably due to the saturation of NO response by endogenous NO in tumors.

Leukocyte-Endothelial Interaction

Low leukocyte-endothelial interaction in tumor vessels[15] is considered as one of the major limitations of immune therapy or host immune response against tumors. Systemic injection of L-NAME significantly increased both leukocyte rolling and stable adhesion to the vessel wall in MCaIV and LS174T tumors, suggesting a possible role for NO in regulating leukocyte-endothelial interactions. The mechanisms for how NO down-regulates leukocyte-endothelial interactions in tumors are still unknown. Tumor cells are known to produce various cytokines or growth factors that can modify the expression of adhesion molecules.[32] Both the production of these mediators and the expression of adhesion molecules are tumor dependent.[33] A lower response to inflammatory mediators in tumor vessels has been reported.[15,33] Reduced expression of adhesion molecules could be an explanation for low level of leukocyte-endothelial interactions in tumors. Davenpeck et al[34] reported P-selectin up-regulation in vessels of rat mesentery after NO inhibition, and Kubes et al[6] reported the involvement of CD18/ICAM-1 in the NO inhibition-mediated increase in leukocyte-endothelial interactions after ischemia-reperfusion. Caterina et al reported that NO donors decreased cytokine-induced VCAM-1 expression and monocyte adhesion on human endothelial cells.[35] These studies of normal vessels and endothelial cells are consistent with our new findings in leukocyte-endothelial interactions in tumors. Low leukocyte flux was reported in angiogenic vessels, and this might be another reason for the low level of leukocyte-endothelial interactions in tumors.[36] However, MCaIV tumor is an exception, where leukocyte flux in MCaIV tumor is comparable to host vessels.[15] In this study, NO inhibitor did not significantly change leukocyte flux in both MCaIV and LS174T tumor vessels but decresed V_{RBC}. Thus, shear rate was significantly decreased in both tumors. The decrease in shear stress could also ac-

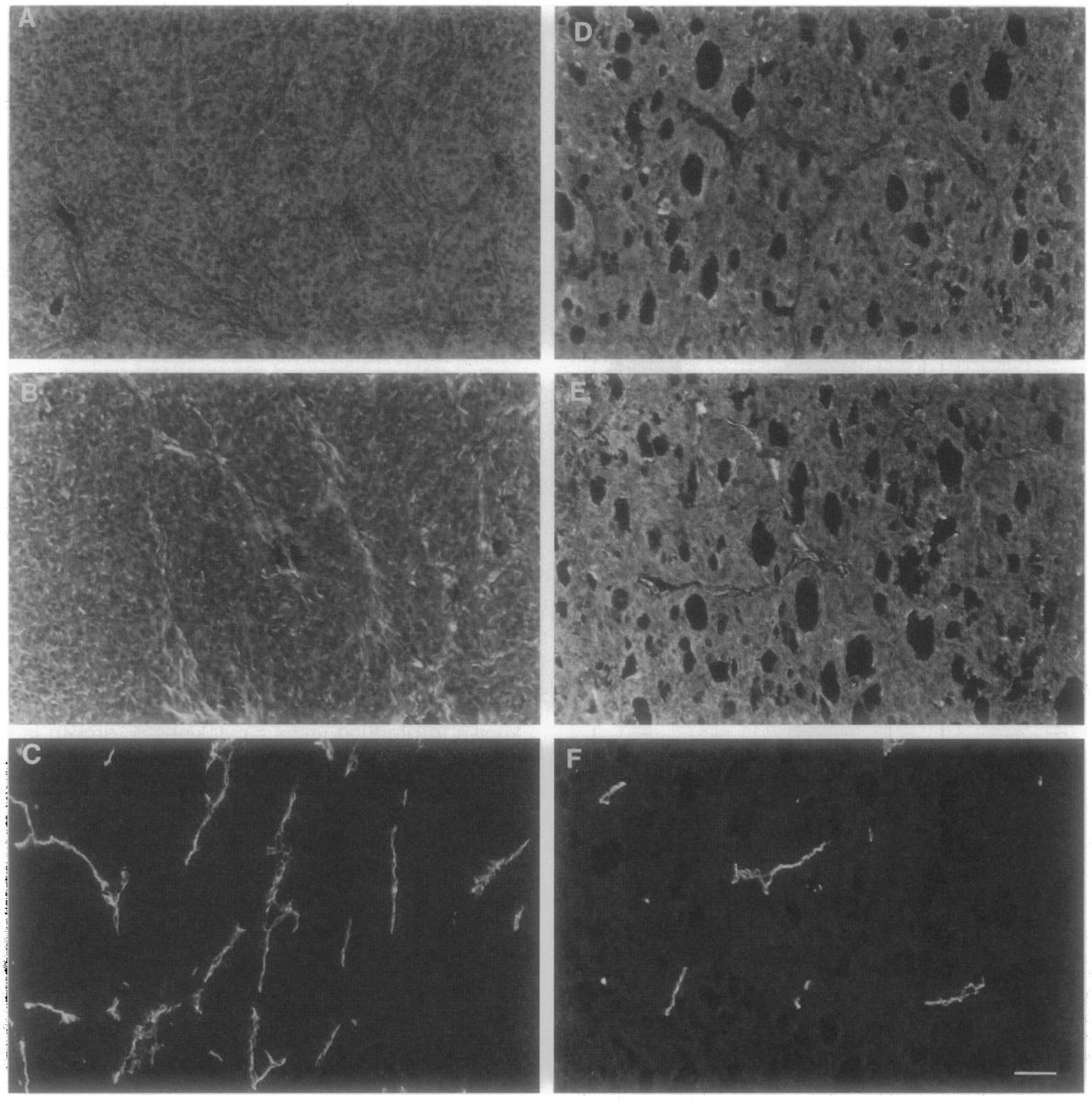

Figure 5. *Immunohistochemical observation of MCaIV and LS174T tumors. Immunolabeling with a polyclonal antibody to eNOS revealed diffuse pattern of positive staining in both MCaIV* (A) *and LS174T* (D) *tumors. Immunolabeling with a polyclonal antibody to iNOS revealed a slightly stronger, diffuse staining than eNOS in both tumors* (B *and* E). *CD31 staining for vascular endothelial cells was positive in both tumors* (C *and* F). A *to* C: *MCaIV tumor.* D *to* F: *LS174T tumor.* A *and* D: *eNOS.* B *and* E: *iNOS.* C *and* F: *CD31 staining. Bar, 100 μm. All photos have the same magnification.*

count for the increase in leukocyte-endothelial interactions induced by NO inhibition.

Vascular Permeability

Many studies have documented the role of NO in microvascular permeability regulation.[37] However, the results are contradictory. Kubes et al[38] and Filep et al[39] reported that NOS inhibitor L-NAME increased microvascular leakage to protein in various tissues including stomach, intestine, liver, spleen, pancreas, kidney, and lung, whereas Yuan et al[40] and Maeda et al[13] reported that NO inhibitor decreased microvascular permeability of coronary venules and sarcoma vessels, respectively. NOS inhibition also affects inflammatory mediator-induced alteration in microvascular permeability. NOS inhibitor decreases histamine, leukotrien C_4-, ADP-, bradykinin-, substance-P-, endotoxin-, 5-hydroxytryptamine-, and platelet-activating factor-induced permeability changes,[28,37,41–43] whereas it augments PAF-, serotonin-, and ischemia-reperfusion-induced increase

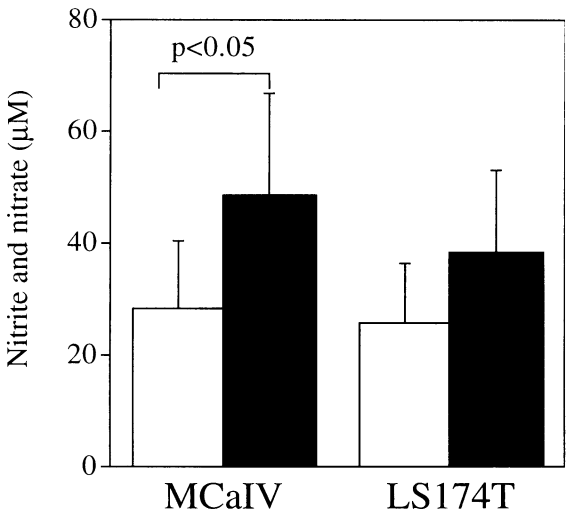

Figure 6. *Nitrite and nitrate levels in interstitial fluid. Nitrite and nitrate levels in tumor interstitial fluid of MCaIV tumor (n = 18) were significantly higher than that in subcutaneous interstitial fluid of non-tumor-bearing C3H mice (n = 9), whereas there was insignificant difference in NO production between LS174T tumors (n = 14) and the host normal tissues (n = 8). □, normal subcutaneous interstitial fluid; ■, tumor interstitial fluid. Data are presented as mean ± SD.*

in vascular permeability.[37–39] The role of NO in regulating vascular permeability is thus different among different tissues and/or species.

In general, tumor vascular permeability is higher than that of normal host vessels.[20,44] The structure of tumor vascular wall is different from that of normal vessels. Vascular endothelial growth factor/vascular permeability factor,[45] bradykinin,[46] tumor necrosis factor-α,[47] interleukin-2,[47] and NO[13] are potent inducers of high vascular permeability in tumors and these mediators also interact with each other.[28] The role of NO in the regulation of tumor vascular permeability seems to be tumor dependent. In this study, L-NAME reduced vascular permeability of MCaIV but not LS174T tumors. The permeability results are consistent with the measurement of nitrite and nitrate levels in tumor interstitial fluid; NO was more abundant in MCaIV than in LS174T.

The accumulation of adherent leukocytes in venules after endogenous NO inhibition was not accompanied by a further increase in vascular permeability. Our hypothesis is that high vascular permeability in tumors is not likely to be leukocyte dependent as in inflammatory processes in normal tissue because of high expression of vascular endothelial growth factor in tumors.[45] Vascular endothelial growth factor is much more potent than inflammatory agents (eg, histamine) in terms of increasing the vascular permeability.[48] Furthermore, leukocytes could be inactivated by cytokines such as transforming growth factor-β1 present in the tumor microenvironment.[49] Finally, direct effect of NO inhibitor on tumor vasculature could overwhelm the changes induced by leukocyte adhesion.

The results of this study suggest that endogenous NO increases/maintains tumor blood flow *via* dilatation of arteriolar vessels, decreases leukocyte-endothelial interactions, and increases vascular permeability in some tumors. The magnitude of the

Table 2. *NO Production and NOS in Tumors*

Tumor	Methods	Results	Reference
NO production in tumor			
Colon 26 B16 melanoma	NOS activity	cNOS (−), iNOS (25–27 pmol/minute/mg)	24
Human gynecological cancer	NOS activity	NOS (<15–1950 pmol/minute/g tissue)	26
Human breast cancer	NOS activity NO_2/NO_3 in tissue culture	NOS (5.1 ± 1.4 pmol/minute/mg protein) NO_2/NO_3 (1.9 ± 0.45 nmol/mg protein/24 hours)	25
MCaIV LS174T	NO_2/NO_3 in TIF	MCaIV, NO_2/NO_3 48.3 ± 18.6 μmol/L LS174T, NO_2/NO_3 38.1 ± 14.9 μmol/L	This work
Immunohistochemistry			
Colon 26, B16		cNOS (−), iNOS (+, vasc.)	24
Human CNS tumors		nNOS (+, tumor), eNOS (+, tumor, vasc.), iNOS (±)	27
Human gynecological cancers		cNOS (+, tumor), iNOS (−)	26
Human breast cancers		cNOS (+, vasc, MØ, Myoepithelial cell), iNOS (+, MØ)	25
RG2 rat glioma		nNOS (+, tumor), eNOS (+, tumor, vasc.)	28
MCaIV murine mammary adenocarcinoma LS174T human colon adenocarcinoma		eNOS (+, tumor), iNOS (+, tumor) eNOS (+, tumor), iNOS (+, tumor)	This work

cNOS, constitutive NOS; NO_2/NO_3, nitrite and nitrate level; TIF, tumor interstitial fluid; vasc., vasculature; MØ, macrophage.

response to NO and/or the production of NO in tumors is tumor dependent. Improvement of blood flow and increase in vascular permeability facilitate supply of nutrients and oxygen to tumor cells, and a decrease in leukocyte-endothelial interactions can help to circumvent host immune attack. These functions of NO in tumors potentially facilitate tumor growth.[50,51]

According to the results of this study and previous reports, modulation of NO levels in tumors can be a useful strategy for alteration of tumor hemodynamics, leukocyte-endothelial interactions, and vascular permeability, which in turn may improve delivery of oxygen, drugs, gene vectors, and effector cells to tumors.

Acknowledgments

We thank Julia Kahn and Yi Chen for dorsal skin chamber preparations, Sylvie Roberge for Gullino's chamber preparations, Dr. Dennis Brown for help with the immunohistochemical studies, and Drs. Axel Sckell and Paul Huang for their helpful comments.

References

1. Moncada S: The L-arginine: nitric oxide pathway. Acta Physiol Scand 1992, 145:201–227
2. Ignaro LJ: Endothelium-derived nitric oxide: actions and properties. FASEB J 1989, 3:31–36
3. Bertuglia S, Colantuoni A, Intaglietta M: Capillary reperfusion after L-arginine, L-NMMA, and L-NNA treatment in cheek pouch microvasculature. Microvasc Res 1995, 50:162–174
4. Sneddon JM, Vane JR: Endothelium-derived relaxing factor reduces platelet adhesion to bovine endothelial cells. Proc Natl Acad Sci USA 1988, 85:2800–2804
5. McCall TB, Boughton-Smith NK, Palmer RM, Whittle BJ, Moncada S: Synthesis of nitric oxide from L-arginine by neutrophils: release and interaction with superoxide anion. Biochem J 1989, 261:293–296
6. Kubes P, Suzuki M, Granger DN: Nitric oxide: an endogenous modulator of leukocyte adhesion. Proc Natl Acad Sci USA 1991, 88:4651–4655
7. Hibbs JB, Taintor RR, Vavrin Z, Rachlin EM: Nitric oxide: a cytotoxic activated macrophage effector molecule. Biochem Biophys Res Commun 1988, 157:87–94
8. Fukumura D, Yonei Y, Kurose I, Saito H, Higuchi H, Miura S, Kato S, Kimura H, Ebinuma H, Ishii H: Role of nitric oxide in Kupffer cell-mediated hepatoma cell cytotoxicity *in vitro* and *ex vivo*. Hepatology 1996, 24: 141–149
9. Andrade SP, Hart IR, Piper PJ: Inhibition of nitric oxide synthase selectively reduces flow in tumour-associated neovasculature. Br J Pharmacol 1992, 107:1092–1095
10. Wood PJ, Sansom JM, Butler SA, Stratford IJ, Cole SM, Szabo C, Thiemermann C, Adams GE: Induction of hypoxia in experimental murine tumors by the nitric oxide synthase inhibitor, N^G-nitro-L-arginine. Cancer Res 1994, 54:6458–6463
11. Tozer GM, Prise VE, Bell KM: The influence of nitric oxide on tumour vascular tone. Acta Oncol 1995, 34: 373–377
12. Meyer RE, Shan S, DeAngelo J, Dodge RK, Bonaventura J, Ong ET, Dewhirst MW: Nitric oxide synthase inhibition irreversibly decreases perfusion in the R3230AC rat mammary adenocarcinoma. Br J Cancer 1995, 71:1169–1174
13. Maeda H, Noguchi Y, Sato K, Akaike T: Enhanced vascular permeability in solid tumor is mediated by nitric oxide and inhibited by both new nitric oxide scavenger and nitric oxide synthase inhibitor. Jpn J Cancer Res 1994, 85:331–334
14. Leunig M, Yuan F, Menger MD, Boucher Y, Goetz AE, Messmer K, Jain RK: Angiogenesis, microvascular architecture, microhemodynamics, and interstitial fluid pressure during early growth of human adenocarcinoma LS174T in SCID mice. Cancer Res 1992, 52: 6553–6560
15. Fukumura D, Salehi HA, Witwer B, Tuma RF, Melder RJ, Jain RK: Tumor necrosis factor-α-induced leukocyte adhesion in normal and tumor vessels: effect of tumor type, transplantation site, and host strain. Cancer Res 1995, 55:4824–4829
16. Southwick PL, Ernst LA, Tauriello EW, Parker SR, Mujumdar RB, Mujumdar SR, Clever HA, Waggoner AS: Cyanine dye labeling reagents: carboxymethylindocyanine succinimidyl esters. Cytometry 1990, 11: 418–430
17. Villringer A, Dirnagl U, Them A, Shurer L, Krombach F, Einhaul KM: Imaging of leukocytes within the rat brain cortex *in vivo*. Microvasc Res 1991, 42:305–315
18. Lipowsky HH, Zweifach BW: Technical report: applications of the "two-slit" photometric technique to the measurement of microvascular volumetric flow rates. Microvasc Res 1978, 15:93–101
19. Yuan F, Salehi HA, Boucher Y, Vasthare US, Tuma RF, Jain RK: Vascular permeability and microcirculation of gliomas and mammary carcinomas transplanted in rat and mouse cranial window. Cancer Res 1994, 54: 4564–4568
20. Yuan F, Leunig M, Berk DA, Jain RK: Microvascular permeability of albumin, vascular surface area, and vascular volume measured in human adenocarcinoma LS174T using dorsal chamber in SCID mice. Microvasc Res 1993, 45:269–289
21. Brizel DM, Klitzman B, Cook JM, Edwards J, Rosner G, Dewhirst MW: A comparison of tumor and normal tissue microvascular hematocrits and red cell fluxes in a rat window chamber model. Int J Radiat Oncol Biol Phys 1993, 25:269–276
22. Valenti G, Verbavatz JM, Sabolic I, Ausiello DA, Verkman AS, Brown D: A basolateral CHIP28/MIP26-related protein (BLIP) in kidney principal cells and gastric parietal cells. Am J Physiol 1994, 267:C812–C820

23. Gullino PM: Techniques in tumor pathophysiology. Methods in Cancer Research. Edited by H Busch. New York, Academic Press, 1970, pp 45–91
24. Buttery LDK, Spingall DR, Andrade SP, Riveros-Moreno V, Hart I, Piper PJ, Polak JM: Induction of nitric oxide synthase in the neo-vasculature of experimental tumors in mice. J Pathol 1993, 171:311–319
25. Thomsen LL, Miles DW, Happerfield L, Bobrow LG, Knowles RG, Moncada S: Nitric oxide synthase activity in human breast cancer. Br J Cancer 1995, 72:41–44
26. Thomsen LL, Lawton FG, Knowles RG, Beesley JE, Riveros-Moreno V, Moncada S: Nitric oxide synthase activity in human gynecological cancer. Cancer Res 1994, 54:1352–1354
27. Cobbs CS, Brenman JE, Aldape KD, Bredt DS, Israel MA: Expression of nitric oxide synthase in human central nervous system tumors. Cancer Res 1995, 55:727–730
28. Nakano S, Matsukado K, Black KL: Increased brain microvessel permeability after intracarotid bradykinin infusion is mediated by nitric oxide. Cancer Res 1996, 56:4027–4031
29. Jain RK: Determinants of tumor blood flow: a review. Cancer Res 1988, 48:2641–2658
30. Warren BA: The vascular morphology of tumors. Tumor Blood Circulation. Edited by H-I Peterson. Boca Raton, FL, CRC Press, 1979, pp 1–48
31. Tanda S, Patan S, Roberge S, Jones RC, Jain RK: Distribution of contractile elements in tumor vessels. Int J Microcirc Clin Exp 1996, 16(S1):150
32. Melder RJ, Koenig GC, Witwer BP, Safabakhsh N, Munn LL, Jain RK: During angiogenesis, vascular endothelial growth factor and basic fibroblast growth factor regulate natural killer cell adhesion to tumor endothelium. Nature Med 1996, 2:992–997
33. Jain RK, Koenig GC, Dellian M, Fukumura D, Munn LL, Melder RJ: Leukocyte-endothelial adhesion and angiogenesis in tumors. Cancer Metastasis Rev 1996, 15: 195–204
34. Davenpeck KL, Gauthier TW, Lefer AM: Inhibition of endothelial-derived nitric oxide promotes P-selectin expression and actions in the rat microcirculation. Gastroenterology 1994, 107:1050–1058
35. Caterina RD, Libby P, Peng H-B, Thannickal VJ, Rajavashisth TB, Gimbrone MAJ, Shin WS, Liao JK: Nitric oxide decreases cytokine-induced endothelial activation. J Clin Invest 1995, 96:60–68
36. Dellian M, Witwer BP, Salehi HA, Yuan F, Jain RK: Quantitation and physiological characterization of angiogenic vessels in mice: effect of basic fibroblast growth factor, vascular endothelial growth factor/vascular permeability factor, and host microenvironment. Am J Pathol 1996, 149:59–72
37. Kubes P: Nitric oxide affects microvascular permeability in the intact and inflamed vasculature. Microcirculation 1995, 2:235–244
38. Kubes P, Granger D: Nitric oxide modulates microvascular permeability. Am J Physiol 1992, 262:H611–H615
39. Filep JG, Földes-Filep E: Modulation by nitric oxide of platelet-activating factor-induced albumin extravasation in the conscious rat. Br J Pharmacol 1993, 110: 1347–1352
40. Yuan Y, Granger HJ, Zawieja DC, DeFily DV, Chilian WM: Histamine increases venular permeability *via* a phospholipase C-NO synthase-guanylate cyclase cascade. Am J Physiol 1993, 264:H1734–H1739
41. Boughton-Smith NK, Evans SM, Laszlo F, Whittle BJR, Moncada S: The induction of nitric oxide synthase and intestinal vascular permeability by endotoxin in the rat. Br J Pharmacol 1993, 110:1189–1195
42. Fujii E, Irie K, Uchida Y, Tsukahara F, Muraki T: Possible role of nitric oxide in 5-hydroxytryptamine-induced increase in vascular permeability in mouse skin. Naunyn-Schmiedeberg's Arch Pharmacol 1994, 350:361–364
43. Ramírez MM, Quardt SM, Kim D, Oshiro H, Minnicozzi M, Durán WN: Platelet activating factor modulates microvascular permeability through nitric oxide synthesis. Microvasc Res 1995, 50:223–234
44. Jain RK: Transport of molecules across tumor vasculature. Cancer Metastasis Rev 1987, 6:559–593
45. Senger DR, Galli SJ, Dvorak AM, Perruzzi CA, Harrey VS, Dvorak HF: Tumor cells secrete a vascular permeability factor that promotes accumulation of ascitic fluid. Science 1983, 219:983–985
46. Matsumura Y, Kimura M, Yamamoto T, Maeda H: Involvement of the kinin-generating cascade in enhanced vascular permeability in tumor tissue. Jpn J Cancer Res 1988, 79:1327–1334
47. Ettinghausen SE, Puri RJ, Rosenberg SA: Increased vascular permeability in organs mediated by the systemic administration of lymphokine-activated killer cells and recombinant interleukin-2 in mice. J Natl Cancer Inst 1988, 80:177–187
48. Dvorak HF, Brown LF, Detmar M, Dvorak AM: Vascular permeability factor/vascular endothelial growth factor, microvascular hyperpermeability, and angiogenesis. Am J Pathol 1995, 146:1029–1039
49. Smith WB, Noack L, Khew-Goodall Y, Isenmann S, Vadas MA, Gamble JR: Transforming growth factor-β1 inhibits the production of IL-8 and the transmigration of neutrophils through activated endothelium. J Immunol 1996, 157:360–368
50. Orucevic A, Lala PK: *NG*-Nitro-L-arginine methyl ester, an inhibitor of nitric oxide synthesis, ameliorates interleukin 2-induced capillary leakage and reduces tumour growth in adenocarcinoma-bearing mice. Br J Cancer 1996, 73: 189–196
51. Jenkins DC, Charles IG, Thomsen LL, Moss DW, Holmes LS, Baylis SA, Rhodes P, Westmore K, Emson PC, Moncada S: Role of nitric oxide in tumor growth. Proc Natl Acad Sci USA 1995, 92:4392–4396